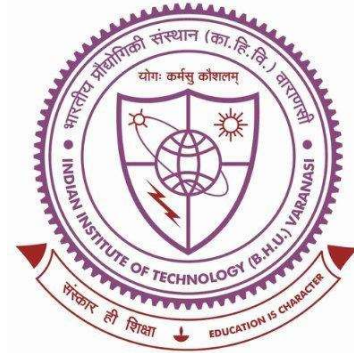


On the Assessment of Nano-oils for Medium-temperature Solar Thermal Systems



A thesis submitted in partial fulfillment for the
Award of Degree

Doctor of Philosophy

By

Satish Upadhyay

**DEPARTMENT OF MECHANICAL ENGINEERING
INDIAN INSTITUTE OF TECHNOLOGY
(BANARAS HINDU UNIVERSITY)
VARANASI-221005
INDIA**

18131006

2023

CERTIFICATE

It is certified that the work contained in the thesis titled “**On the Assessment of Nano-oils for Medium-temperature Solar Thermal Systems**” by Satish Upadhyay has been carried out under our supervision and that this work is not submitted elsewhere for any degree.

It is further certified that the student has satisfactorily fulfilled all the requirements of the Comprehensive Examination, Candidacy, SOTA, and Pre-submission seminar for the award of the Ph.D. degree.



Dr. Laltu Chandra (Ex-Faculty)

(Supervisor)

Department of Mechanical Engineering

IIT (BHU), Varanasi-221005

*Associate Professor
Deptt. of Mechanical Engg.
Indian Institute of Technology (BHU)
Varanasi-221005*

Prof. Jahar Sarkar

(Supervisor)

Department of Mechanical Engineering

IIT (BHU), Varanasi-221005

*प्राध्यापक / Professor
यान्त्रिक अभियान्तिकी विभाग / Deptt. of Mechanical Engg.
भारतीय प्रौद्योगिकी संस्थान / Indian Institute of Technology
(कांठिगंज / B.H.U.)
वाराणसी-२२१००५ / Varanasi-221005*

DECLARATION BY THE CANDIDATE

I, "Satish Upadhyay," certify that the work embodied in this thesis is my bonafide work and was carried out by me under the supervision of **Dr. Laltu Chandra** and **Prof. Jahar Sarkar** from "2018" to "2023", at the **Department of Mechanical Engineering, Indian Institute of Technology (BHU), Varanasi**. The matter embodied in this thesis has not been submitted for the award of any other degree. I declare that I have faithfully acknowledged and given credits to the research workers wherever their works have been cited in my work in this thesis. I further declare that I have not willfully copied any other's work, paragraphs, text, data, results, etc., reported in journals, books, magazines, reports, dissertations, theses, etc., or available at websites and have not included them in this thesis and have not cited as my work.

Date: 24/04/2023

Place: Varanasi


Satish Upadhyay

(Candidate)

CERTIFICATE BY THE SUPERVISOR(S)

It is certified that the above statement made by the student is correct to the best of my/our knowledge.


Dr. Laltu Chandra (Ex-Faculty)

(Supervisor) Professor
Deptt. of Mechanical Engg.
Indian Institute of Technology (BHU)
Varanasi-221005


Head of the Department


पाठ्यप्रोफेसर / Professor
Prof. Jahar Sarkar
यांत्रिक अभियान्त्रिकी विभाग / Deptt. of Mechanical Engg.
भारतीय प्रौद्योगिकी संस्थान (Supervisor) Indian Institute of Technology
(काठिंडी/वि०/B.H.U.)
वाराणसी-२२१००५ / Varanasi-221005

Mechanical Engineering Department, IIT (BHU), Varanasi

विभागाध्यक्ष / HEAD
यांत्रिकी अभियान्त्रिकी विभाग / Deptt. of Mechanical Engg.
भारतीय प्रौद्योगिकी संस्थान / Indian Institute of Technology
(काठिंडी/वि०/B.H.U.)
वाराणसी-२२१००५ / Varanasi-221005

COPYRIGHT TRANSFER CERTIFICATE

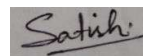
Title of the Thesis: On the Assessment of Nano-oils for Medium-temperature Solar Thermal Systems.

Candidate's Name: Satish Upadhyay

COPYRIGHT TRANSFER

The undersigned hereby assigns to the Institute of Technology (Banaras Hindu University) Varanasi all rights under copyright that may exist in and for the above thesis submitted for the award of the Ph.D. degree.

Date: 24/04/2023



Place: IIT (BHU), Varanasi

(Satish Upadhyay)

Note: However, the author may reproduce or authorize others to reproduce material extracted verbatim from the thesis or derivative of the thesis for the author's personal use provided that the source and the Institute's copyright notice are indicated.

ACKNOWLEDGEMENTS

I take this opportunity to express my deep sense of gratitude to my supervisor, **Dr. Laltu Chandra**, and **Prof. Jahar Sarkar**, for their continuous guidance and whole-hearted cooperation in carrying out this work. His thorough and valuable review and constructive criticism of the chapter have greatly improved the quality of the work. Sir, your faith in me and the desire to live up to your expectations have constantly pushed me to work harder.

I also thank **Prof. Pradyumna Ghosh** and **Dr. J. P. Chakraborty** for serving on my research progress evaluation committee (RPEC). Thank you all for sparing your valuable time and assisting me throughout my research and completion of this thesis. I sincerely thank Prof. Santosh Kumar, Head of the Department of Mechanical Engineering, for providing me with the necessary resources to complete this research work. During my stay at IIT (BHU) Varanasi, I met many people who have made this period of my life memorable and very pleasant. Among them, I sincerely acknowledge the assistance and motivation provided by **Dr. Rashmi Rekha Sahoo**, **Dr. Swasti Sundar**, **Dr. Om Prakash Singh**, and **Dr. Amitesh Kumar**. I want to thank my colleagues at IIT (BHU) Varanasi, especially **Mr. Mayaram Sahu**, **Mrs. Archana Kumari**, **Mr. Mayank Srivastava**, **Mr. Jayprakash**, **Mr. Sarvesh Yadav**, **Mr. Prashant Srivastava**, **Mr. Vinay Kumar Yadav**, **Mr. Praveen Kumar**, and **Mr. Rishi Ram** for encouraging me to finish this work.

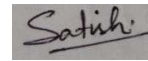
The experimental part of this thesis has been carried out at the Department of Mechanical Engineering IIT (BHU) Varanasi. Several persons have assisted and supported me in designing and developing the test rig. I sincerely thank **Mr. Moolchand**, **Mr. Sunil Bardhan**, and **Mr. Barmeshwar Prasad** for giving valuable ideas while performing experiments and providing the measurement tools and instruments whenever needed for the research work without any hesitation.

I would like to acknowledge my parents, especially my elder brother **Dr. Deep Chandra Upadhyay**, my wife **Aradhana Tiwari** and family for not engaging me in any other affairs during my research duration and handling all the matters alone. I thank my parents for assisting me financially whenever needed and motivating me in my work. Your sacrifices for allowing me to devote my attention to my research work entirely are greatly acknowledged and appreciated.

I would also like to thank GOD the Almighty for giving me the strength to remain on the path to success.

Date:24/04/2023

Place: IIT (BHU), Varanasi



(Satish Upadhyay)

TABLE OF CONTENTS

CERTIFICATE	i
DECLARATION BY THE CANDIDATE	ii
COPYRIGHT TRANSFER CERTIFICATE.....	iii
ACKNOWLEDGEMENTS.....	iv
TABLE OF CONTENTS.....	vi
LIST OF TABLES	x
LIST OF FIGURES	xii
LIST OF SYMBOLS	xviii
ABSTRACT.....	xxi
Chapter 1: Introduction	1
1.1 Background and Motivation	1
1.2 Objectives and Novelty of the Thesis.....	5
1.3 Thesis Structure	6
Chapter 2: Literature Review.....	7
2.1 PTC Absorber: Heat Transfer and Heat Transfer Fluids.....	7
2.2 Nusselt Number Correlation: Pure and Nanofluids	11
2.3 PTC Absorber: Discrete Heating.....	14
2.4 Research Gaps	16
Chapter 3: A Generalized Nusselt Number Correlation for Nanofluids and Look-up Diagram to Select Heat Transfer Fluids.....	17

3.1	Selection Criteria for Heat Transfer Fluids	17
3.1.1	Dimensional and Non-dimensional Parameters	17
3.1.2	Pure Fluids	20
3.1.3	Nanofluids	23
3.2	Results and Discussion	35
3.2.1	Improved Nusselt Number Correlation for Nanofluids	35
3.2.2	Heat Transfer Fluid Selection: Dimensional Parameter	40
3.2.3	Heat Transfer Fluid Selection: Non-dimensional Figure of Merit.....	42
3.2.4	Heat Transfer Fluid Selection: Look-up Diagrams.....	44
3.2.5	Heat Transfer Fluid: Cost-benefit Analysis	48
3.3	Summary.....	49
Chapter 4: A Generalized Nusselt Number Correlation for Binary Hybrid Nano-oils as Heat Transfer Fluid.....		51
4.1	Hybrid Nanofluids	51
4.1.1	Nusselt Number Correlations for Hybrid Nanofluids: A Comparative Assessment	52
4.1.2	Separation Approach: Generalized Nusselt Correlation for Hybrid Nanofluids	54
4.2	CFD Analysis: Turbulent Forced Convection	55
4.2.1	Problem Description	56
4.2.2	Mathematical Modeling	58
4.2.3	Boundary Conditions and Numerical Scheme	60

4.2.4	Grid Independence Test and Validation	61
4.3	Results and Discussion	65
4.3.1	Hydro-Thermal Development of Turbulent Oil Flow	65
4.3.2	Separation-based Nu_{gen} : Need and Assessment	67
4.4	Summary.....	71
Chapter 5: New Insights in Turbulent Heat Transfer with Oil and Hybrid Nano-oils, Subject to Discrete Heating, for Parabolic Trough Absorbers		
5.1	Computational Fluid Dynamics Framework	73
5.1.1	Problem Description	73
5.1.2	Mathematical Modeling.....	76
5.1.3	Grid Independence Test and Validation	80
5.2	Results and Discussion	82
5.2.1	Axial Velocity Contour.....	83
5.2.2	Radial Distribution of the Axial Velocity.....	86
5.2.3	Streamline	92
5.2.4	Temperature Contour	93
5.2.5	Radial Distribution of Statistical Temperature for TVP1	98
5.2.6	Surface-Area-Averaged Nusselt Number for Oil and Hybrid Nano-Oils..	102
5.3	Summary.....	106
Chapter 6: Experimental study with a Hybrid Nano-Oil for Assessing the Generalized Nusselt Number Correlation		
6.1	Experimental Setup and Procedure.....	109

6.1.1	Hybrid Nano-Oil Preparation: Al ₂ O ₃ -Cu _o TVP1	113
6.1.2	Data Deduction	115
6.1.3	Uncertainty Analysis.....	116
6.1.4	Validation.....	117
6.2	Results and Discussion	118
6.2.1	Hybrid Nanofluid: Stability	118
6.2.2	Convective Heat Transfer Coefficient and Nusselt Number: Oil and Hybrid Nano-oil.....	119
6.2.3	Pressure drop and Friction Factor: Oil and Hybrid Nano-oil	120
6.2.4	Nusselt Number and Figure of Merit: Oil and Hybrid Nano-oil	120
6.3	Summary.....	121
Chapter 7: Conclusions and Future Work.....		123
REFERENCES		127
LIST OF PUBLICATIONS AND CONFERENCES		145

LIST OF TABLES

Table 1.1 Solar thermal systems, applications, and their operating conditions.....	2
Table 2.1 Nusselt number correlations for pure and mono-dispersed nanofluids	11
Table 2.2 Nusselt number correlations for hybrid nanofluids.	13
Table 3.1 Dimensional and non-dimensional parameters.....	19
Table 3.2 Heat transfer fluid (HTF) composition, thermophysical properties, and temperature range.....	21
Table 3.3 Parameters to define the shapes of nanoparticles [100].....	25
Table 3.4 Thermophysical properties of nanoparticles.....	26
Table 3.5 The collected experimental data for Nu_{NF} with different nanoparticle types, shapes and concentrations.....	34
Table 3.6 Estimated coefficients C_1 to C_4 using Dittus-Boelter and Gnielinski correlations for Nu_{BF}	39
Table 3.7 Analysis of dimensional parameters as in Table 3.1.	40
Table 3.8 Cost of heat transfer fluids and their benefit for practical applications [117]. ..	48
Table 4.1 The generated grids and calculated Nu using CFD modeling.	57
Table 4.2 The adopted coefficients for CFD simulation with the SKE model [125].	60
Table 4.3 The computed coefficients for η using the experimental Nu_{hnf} and R^2 value.....	68

Table 5.1 The applied heat fluxes on the top and bottom surfaces of the tube for CFD analyses	75
Table 5.2 The adopted thermophysical properties of fluids and solids for CFD analyses	77
Table 5.3 Mass flow rate through the upper and lower half of the cross-section, at various axial locations, including the effect of gravity, and for $q_r = 1$, at $Re = 5000$	87
Table 5.4 The RANS-analyzed wall shear stress (τ in Pa).....	91
Table 6.1 The measured parameters, instruments, and their operating range/accuracy ..	111
Table 6.2 Uncertainty estimation for different experiment-based parameters	116

LIST OF FIGURES

Figure 1.1 A schematic of the solar-based heating and cooling system: 1: Solar collector with a receiver, 2: Thermal energy storage, 3 & 4: Heat exchangers, 5: Valve, and 6: Pump.3

Figure 1.2 a) Solar energy flow diagram and distribution in the Parabolic Trough Collector –Secondary Reflector (PTC-SR) [10] b)Comparison of circumferential flux distribution on absorber surface for different secondary reflector designs for PTC [10].4

Figure 3.1 A comparison between Nu_{NF} correlations for nanofluids with (a) spherical (CuO)29

Figure 3.2 A separation approach to obtain Nu_{NF} for nanofluids using Nu_{BF} for base fluid and the correction factor (η) for nanoparticles.33

Figure 3.3 A comparison between correlation in equation 3.9 and experiment-based Nu_{NF} for (a) CuO-water ($\phi= 0.015 - 0.236 \%$),and (b) CNT-water ($\phi=0.0236-0.095 \%$) nanofluids.37

Figure 3.4 A comparison between correlation and experimental Nu_{NF} with different Cu-water, CuO-water, TiO₂-water, CNT-water, GNP-water, Al₂O₃-water, and MgO-water nanofluids. Refer to Table 3.5 for their properties.....38

Figure 3.5 A comparative assessment of the non-dimensional figure of merit at (a) 453K and (b) 573K with different pure fluids, nanofluids, and hybrid nanofluids for $\phi = 0.2\%$44

Figure 3.6 A qualitative look-up diagram for the selection of a heat transfer fluid, including nanofluids and hybrid nanofluids, for a temperature range of 373-573 K.....	45
Figure 3.7 A Mollier-type quantitative look-up diagram for the selection of a heat transfer fluid.....	46
Figure 4.1 Comparison of water-based Nu_{hnf} for (a) ND-Ni (spherical-spherical) (b) MWCNT-Fe ₃ O ₄ (cylindrical-spherical), (c) rGO-Co ₃ O ₄ (platelet-spherical) nanoparticles for $2300 < Re_{hnf} < 22000$, $4 < Pr_{hnf} < 8$ and $20\text{ }^{\circ}\text{C} < T < 80\text{ }^{\circ}\text{C}$	54
Figure 4.2 A 2D, axisymmetric schematic of the computational domain for CFD analysis.....	57
Figure 4.3 An example of the generated structured mesh with $y^+ = 1$ for a well-resolved flow field.....	57
Figure 4.4 Variation of thermal conductivity and kinematic viscosity with local bulk mean temperature and input power along the axial direction.....	62
Figure 4.5(a) A comparison between CFD and Choi et al. [123] Nux for $20000 < Re_x < 31000$ and $3 < Pr < 7$, using different turbulence models, at an input power of 9.19 kW, (b) the maximum, relative, percentage deviation between the computed and correlation-based values for Nux , using the different turbulence models, and (c) the computed and correlation-based values for Nux , using the RKE turbulence model and different input powers.....	64
Figure 4.6 A comparison between the computed and correlation-based (Choi and Gnielinski) Nu , for Therminol55 oil with $q'' = 100\text{ kW/m}^2$ and 300 kW/m^2 , $100\text{ }^{\circ}\text{C} < T < 143\text{ }^{\circ}\text{C}$, $11000 < Re_{bf} < 34000$ and $38 < Pr < 44$	65

Figure 4.7 Non-dimensional (a) velocity profiles, (b) zoom-in view of velocity profiles, (c) temperature profiles, and (d) zoom-in view of temperature profiles, for Therminol55 oil with $100\text{ }^{\circ}\text{C} < T < 143\text{ }^{\circ}\text{C}$, $11000 < Re_{bf} < 34000$ and $38 < Pr < 44$66

Figure 4.8 A comparison between CFD and Sundar et al. (2014, 2018) [71][55] for Nu_{hnf} using SiC-TiO₂-diathermic oil and different heat fluxes 100 and 300 kW/m² with $100\text{ }^{\circ}\text{C} < T < 113\text{ }^{\circ}\text{C}$, $10000 < Re_{hnf} < 31000$ and $69 < Pr < 76$68

Figure 4.9 Comparison between the experimental and Nu_{gen} in equation 4.15 for (a) rGO-Co₃O₄-water, and (b) Al₂O₃-Cu-water, GNP-Ag-water, Graphite-SiO₂-water, MWCNT-Fe₃O₄-water, ND-Ni-water, and rGO-Co₃O₄-water for $2300 < Re_{hnf} < 22000$, $20\text{ }^{\circ}\text{C} < T < 80\text{ }^{\circ}\text{C}$ and $4 < Pr_{hnf} < 8$69

Figure 4.10 A comparison of the estimated Nu_{gen} , using case 2 in equation 4.15 with CFD analysed values, for (a) Al₂O₃-TiO₂-Therminol 55 with $100\text{ }^{\circ}\text{C} < T < 130\text{ }^{\circ}\text{C}$, $10000 < Re_{hnf} < 31000$ and $46 < Pr_{hnf} < 54$ and (b) SiC- TiO₂-Diathermic-oil with $100\text{ }^{\circ}\text{C} < T < 113\text{ }^{\circ}\text{C}$, $10000 < Re_{hnf} < 31000$ and $69 < Pr_{hnf} < 76$71

Figure 5.1 Schematic of the 3D straight, long tube with boundaries for computational fluid dynamics analyses.....74

Figure 5.2 Generated structured mesh for 3D computational fluid dynamics analyses. ...76

Figure 5.3 Grid independence test using the time-average, axially varying a) fluid temperature at the centreline and b) the inner wall temperature for $2 \leq z \text{ in m} < 4$81

Figure 5.4 Comparison between (a) CFD analyzed and wall-law for $U +$ with coarse, medium, and fine meshes at $z = 1.9 \text{ m}$ and $Re = 20000$, and (b) CFD analyzed overall,

surface-area-averaged, Nusselt number (Nu_{CFD}) and the Gnielinski correlation $Nu_{Gnielinski}$ for TVP1 with $5000 \leq Re \leq 20000$ and $q_r = 1$	82
Figure 5.5 RANS-based axial velocity contour at the different axial locations for TVP1 with $Re = 5000$, without and with gravity effect ($g = 0$ and 9.81 m/s^2), and different heat flux ratios ($q_r = 1$ and 50).	84
Figure 5.6 RANS-based axial velocity contour at the different axial locations for TVP1 with $Re = 20000$, without and with gravity effect ($g = 0$ and 9.81 m/s^2), and different heat flux ratios ($q_r = 1$ and 50).	86
Figure 5.7 RANS-based axial velocity for simulations without gravity effect and with gravity effect, different Reynolds number $Re = 5000$ and 20000 , and different heat flux ratios $q_r=1$ and 50	89
Figure 5.8 A comparison between the RANS-analyzed non-dimensional axial velocity with the standard logarithmic law at $\theta = 90^0$ and $\theta = 270^0$ for simulations without and with the effect of gravity.....	91
Figure 5.9 The RANS-analyzed streamlines at various axial locations for $q_r = 1$ and $q_r = 50$, considering the effect of gravity at $Re = 5000$	93
Figure 5.10 The RANS-analyzed, statistical, fluid temperature contour at different axial locations for $Re = 5000$, $g = 0$, 9.81 m/s^2 , and different heat flux ratios $q_r = 1$ and 50	96
Figure 5.11 The RANS-analyzed, statistical, fluid temperature contour at different axial locations for $Re = 5000$, $g = 0$, 9.81 m/s^2 , and different heat flux ratios $q_r = 1$ and 50	97

Figure 5.12 (a - h) RANS-based statistic fluid and solid temperatures for simulations without gravity effect and with gravity effect, different Reynolds number $Re = 5000$ and 20000 , and different heat flux ratios $q_r = 1$ and 50101

Figure 5.13 RANS-based (a) fluid and solid temperature for $q_r = 5, 10, 20, 40,$ and 50 simulations with gravity effect at $z = 3.75$ m, $Re = 5000$, and $q_r = 5, 10, 20, 40,$ and 50 . (b) Richardson number using the maximum temperature difference, local thermophysical properties for TVP1, and $Re = 5000$ and 20000 along the axial direction.....101

Figure 5.14 The RANS-based surface-area-averaged Nusselt number (a) for pure TVP1, (b) for Cu-Al₂O₃-TVP1, $1 \leq \phi$ (VV%) ≤ 6 , and (c) is compared with Nu_{gen} for Cu-Al₂O₃-TVP1 with $\phi = 1$ VV%, $q_r = 1$ and 50 . For these simulations, $5000 \leq Re \leq 20000$ and $1 \leq q_r \leq 50$ are selected.....105

Figure 5.15 Comparison of (a) Nub (b) Nut with $Nucorr$ for Cu-Al₂O₃-TVP1 with $\phi = 1$ VV%, and for simulations $5000 \leq Re \leq 20000$ and $5 \leq q_r \leq 50$ are selected.....106

Figure 6.1 Schematic of the installed experiment setup for the heat transfer with therminol and hybrid nano-oil110

Figure 6.2 Photograph of a) the installed experimental setup for heat transfer with oil and hybrid nano-oil, b) the installed, externally insulated heating section with thermocouples, and c) the installed thermocouples at the inlet and outlet to measure fluid temperature. 112

Figure 6.3 Equipment used and steps for the preparation of hybrid nano-oil.....115

Figure 6.4 Comparison of the experiment-based Nusselt number and Friction factor with a) Gnielinski correlation and b) Pethukov correlation for Therminol VP1.117

Figure 6.5 Photograph of a) TVP1, (b)-(f) 1% (V/V) Al₂O₃-CuO-TVP1 hybrid nano-oil starting from day 0 to day 4.118

Figure 6.6 a) Convective heat transfer coefficient and b) Nusselt number for TVP1 and Al₂O₃-CuO-TVP1 hybrid nano-oil.119

Figure 6.7 a) Pressure drop versus volume flow rate, and b) Friction factor versus *Re* for TVP1 and Al₂O₃-CuO-TVP1 hybrid nano-oil.120

Figure 6.8 Comparison between a) experiment-based and generalized Nusselt number for hybrid nano-oil and b) figure of merit for TVP1 and 1% (v/v) of Al₂O₃-CuO-TVP1.....121

LIST OF SYMBOLS

A	model constants	P	pressure (N/m ²)
Bo	Bonilla number	q''	heat flux (W/m ²)
C	constants	q_r	heat flux ratio
c_p	specific heat capacity (J/kg K)	r	radial location (m)
D	tube diameter (m)	Re	Reynolds number
E	the sum of the square of the error	S	modulus of the mean rate of the strain tensor (s ⁻¹)
f	friction factor	T	temperature (K)
G_K	generation of turbulent kinetic energy (kg/m/s ³)	U or V	the velocity of the fluid (m/s)
I	turbulent intensity	u_τ	friction velocity (m/s)
K	Turbulent kinetic energy (m ² /s ²)	y^+	dimensionless wall coordinate
L	tube length (m)	Greek symbols	
Le	Lenert number	θ	Angle (in degree)
M	sample size	α	thermal diffusivity (m ² /s)
Mo	Mouromtseff number	ε	dissipation rate of K (m ² /s ³)
n	Shape factor, constant	ψ	Sphericity
Nu	Nusselt Number	k	thermal conductivity (W/mK)

k_s	Thermal conductivity of solid (W/mK)	RANS	Reynolds-Averaged Stokes	Navier-
ρ	density (kg/m ³)	RKE	Realizable k- ϵ	
σ_K	turbulent Prandtl number for K	SB	Soybean oil	
σ_ϵ	turbulent Prandtl number <i>for</i> ϵ	SKE	standard k- ϵ	
	Abbreviations	SS	Solar salt	
Al ₂ O ₃	Aluminium oxide	TVP1	Therminol VP1 oil	
Al ₂ O ₃ - TiO ₂	Alumina-Titanium oxide	T55	Therminol 55 oil	
CA	Canola oil	T66	Therminol 66 oil	
CFD	Computational fluid dynamics		Subscripts	
CP	Coefficient of Pressure	bf	base fluid or pure fluid	
CST	Concentrated Solar Thermal	b	bottom	
Cu-Al ₂ O ₃	Copper-Alumina oxide	corr	correlation	
FOM	Figure of Merit	gen	generalized	
GNP-Ag	Graphene nanoplatelets-Silver	hnf	hybrid nanofluid	
H	Hitec	i	inner	
HXL	Hitec XL	in	Inlet	
HTF	heat transfer fluid	nf	nanofluid	
MWCNT- Fe ₃ O ₄	Multi-Walled Nanotube	Carbon ns	nanostructure (nanolayer)	
ND-Ni	Nano Diamond –Nickel	o	overall	

out	outer	w	wall
p	nanoparticle	z	axial location (m)
r	ratio	,	the fluctuation from a mean value
s	salt	-	time averaging
t	top		

ABSTRACT

Several industrial process heat applications use fossil fuel-based high-grade energy in the medium-temperature range of 373 – 573 K. There, the use of parabolic trough collector (PTC)-based concentrated solar thermal (CST) system is expected to save fossil fuel, enhance the system efficiency by the direct utilization of heat, and mitigate the emission of greenhouse gases. Such systems rely upon heat transfer fluids (HTFs), including nanofluids, which transport the generated heat from a receiver to the intended applications. However, some of the identified significant challenges for developing such a system are (a) selection of an HTF, including vegetable oils and nano-oils, which can operate in this temperature range, (b) Nusselt number (Nu) correlations are available for pure fluids, and water-based nanofluids for specific nanoparticles, (c) the dearth of experimental data for developing/adopting Nusselt number correlations for nano-oils, and (d) the limitations of the modeling approaches, especially, for analyzing heat transfer with nano-oils in PTC absorber subject to discrete heating. These aspects are addressed in this thesis as follows:

1. A novel *separation approach* is proposed to filter the effect of nanoparticles on the Nu correlation for nanofluids. This leads to a *generalized form of Nu* correlation for nanofluids, which allows the use of a well-accepted Nu correlation for a wide range of the base fluid. The generalized form of Nu correlation for nanofluids predicts the experiment-based Nu for CuO-water, TiO₂-water, Cu-water, and Carbon nanotube-water, primarily within $\pm 20\%$ except for the Graphene nanoplatelet. One way to adopt this approach for hybrid nanofluids is also discussed.
2. A consistent, non-dimensional, figure of merit (FoM) is proposed for pure or nanofluid as HTF in PTC-based CST systems operating in the medium-temperature range. The FoM-based *qualitative* and *quantitative look-up diagrams* are developed

to enable the selection of heat transfer fluids. A comparative assessment shows that the figure of merit for CuO-Canola/TherminolVP1 nano-oil or CuO-Al₂O₃-Canola/TherminolVP1 hybrid nano-oil increases by about 10-30%, in comparison to Canola or TherminolVP1 oil. Therefore, the use of Canola oil and Canola oil-based nano-oil or hybrid nano-oil will be beneficial for solar thermal systems in the medium-temperature range. Moreover, using TherminolVP1-based nano-oil or hybrid nano-oil will benefit concentrated solar thermal power generation systems. A preliminary cost-benefit analysis lends additional support to these findings.

3. Considering the recommendations, arising out of the above findings, heat transfer analyses are performed for the turbulent flow of binary hybrid nano-oils. The investigations lead to extending the proposed generalized Nusselt number correlation for turbulent heat transfer with hybrid nano-oils. Unlike the available water-based, nanoparticle-specific, correlations for the Nusselt number, the developed correlation needs only the thermophysical properties of base fluid and nanoparticles. The generalized Nu correlation for hybrid nanofluids is valid for Reynolds number from 10000 to 30000 and the Prandtl number from 0.5 to 2000. It is found that the proposed correlation predicts the computed and experimental Nu for different hybrid nanofluids, mostly, within $\pm 10-20\%$. However, the need for experiments with hybrid nano-oils is reiterated.
4. It is worth noting that the PTC absorbers are subject to a special type of heating condition, viz., discrete heating. There, the outer periphery's upper half is exposed to direct normal irradiance or reflected part of the direct irradiance, and the lower half of the outer periphery is exposed to the concentrated solar irradiance. This results in a high heat flux ratio between the lower and upper half of the PTC absorber periphery. Therefore, the need for an in-depth understanding of the

turbulent heat transfer in PTC absorbers with pure and hybrid nano-oils, including the effect of buoyancy or gravity, is realized. Thus, the RANS-based turbulent heat transfer analyses in a 3D, long, straight for Reynolds number from 5000 to 20000 and discrete heating conditions with different heat flux ratios such as 1, 5, 10, 20, 40, and 50 for pure oil and hybrid nano-oils having 1, 4 and 6 % volume concentration of the nanoparticles. The major findings are, (a) gravity-induced anisotropy leads to high and low-speed fluid flows near the lower and upper walls and temperature redistribution at a plane, which is beneficial, (b) the statistical axial-velocity deviates from the standard logarithmic law at a Reynolds number of 5000, and (c) the ratio of surface-area-averaged Nusselt number between the lower half and upper half of the tube is 4-12.

5. Finally, experiments with nano-oils are reported to mitigate the dearth of experimental data for assessing the developed generalized Nusselt number correlation. The artificial, Joule-type, uniform heating condition is adopted for simplicity. The major findings are (a) Nusselt number enhances, pressure drop also enhances with the addition of nano-particles, (b) the calculated FoM allows confirming that the use of hybrid nano-oil is beneficial in comparison to pure oil, and (c) the generalized Nu correlations are applicable for hybrid nano-oils within the reported uncertainty of $\pm 15\%$.

